Cellular/Molecular

$P2X_1$ and $P2X_5$ Subunits Form the Functional P2X Receptor in Mouse Cortical Astrocytes

Ulyana Lalo,[1] Yuri Pankratov,[1,2] Sven P. Wichert,[3] Moritz J. Rossner,[3] R. Alan North,[1] Frank Kirchhoff,[3] and Alexei Verkhratsky[1,4]

[1]Faculty of Life Sciences, The University of Manchester, Manchester M13 9PT, United Kingdom, [2]Department of Biological Sciences, University of Warwick, Coventry CV4 7AL, United Kingdom, [3]Department of Neurogenetics, Max Planck Institute of Experimental Medicine, D-37075 Göttingen, Germany, and [4]Institute of Experimental Medicine, Academy of Sciences of the Czech Republic, 142 20 Prague 4, Czech Republic

ATP plays an important role in signal transduction between neuronal and glial circuits and within glial networks. Here we describe currents activated by ATP in astrocytes acutely isolated from cortical brain slices by non-enzymatic mechanical dissociation. Brain slices were prepared from transgenic mice that express enhanced green fluorescent protein under the control of the human glial fibrillary acidic protein promoter. Astrocytes were studied by whole-cell voltage clamp. Exogenous ATP evoked inward currents in 75 of 81 astrocytes. In the majority (~65%) of cells, ATP-induced responses comprising a fast and delayed component; in the remaining subpopulation of astrocytes, ATP triggered a smoother response with rapid peak and slowly decaying plateau phase. The fast component of the response was sensitive to low concentrations of ATP (with EC_{50} of ~40 nM). All ATP-induced currents were blocked by pyridoxal-phosphate-6-azophenyl-2′,4′-disulfonate (PPADS); they were insensitive to ivermectin. Quantitative real-time PCR demonstrated strong expression of $P2X_1$ and $P2X_5$ receptor subunits and some expression of $P2X_2$ subunit mRNAs. The main properties of the ATP-induced response in cortical astrocytes (high sensitivity to ATP, biphasic kinetics, and sensitivity to PPADS) were very similar to those reported for $P2X_{1/5}$ heteromeric receptors studied previously in heterologous expression systems.

Key words: **$P2X_{1/5}$ receptors; cortex; GFAP–EGFP mice; astrocytes; neuron–glial interaction; P2X**

Introduction

Purinergic neurotransmission, prophesied by Geoffrey Burnstock in early 1970s (Burnstock, 1972, 1977, 2004) is now firmly established in both the PNS and CNS (North and Verkhratsky, 2006). ATP-mediated synaptic transmission has been identified in several brain regions *in situ* (Edwards et al., 1992, 1997; Nieber et al., 1997; Pankratov et al., 1998, 2002, 2003, 2006; Mori et al., 2001). ATP also acts as a widespread "glio"transmitter, which mediates reciprocal signaling between neurons and glial cells, as well as an intercellular communication in glial networks (Kirischuk et al., 1995a,b; Cotrina et al., 1998, 2000; Stout et al., 2002; Koizumi et al., 2003; Zhang et al., 2003; Bowser and Khakh, 2004; Fellin et al., 2006; Fields and Burnstock, 2006). Furthermore, ATP released from astroglia may act as important source of adenosine, which exerts additional neurotropic effects via activation of A_1 receptors (Pascual et al., 2005).

ATP triggers cytosolic Ca^{2+} signals or membrane current responses in many types of CNS glia, including astrocytes and radial glia (Salter and Hicks, 1994; Kirischuk et al., 1995b; King et al., 1996), oligodendrocytes (Kirischuk et al., 1995a; James and Butt, 2001), and microglial cells (Haas et al., 1996; Moller et al., 2000; Verderio and Matteoli, 2001; Farber and Kettenmann, 2006). Cellular effects of ATP are mediated through metabotropic P2Y (Erb et al., 2006; Hussl and Boehm, 2006) and ionotropic P2X (Egan et al., 2006) receptors. The importance of P2Y receptors in triggering Ca^{2+} signaling within astroglial networks is well documented (Kirischuk et al., 1995b; Verkhratsky and Kettenmann, 1996; Verkhratsky et al., 1998; Fellin et al., 2006). The functional role and relevance of ionotropic P2X receptors in astroglial signaling remains much less explored, primarily attributable to the absence of functional evidence on P2X receptors types operating in astrocytes *in situ*.

P2X receptors are ATP-gated cationic channels permeable to Na^+, K^+, and Ca^{2+} (Egan et al., 2006; Roberts et al., 2006). The P2X receptor family includes seven subunits ($P2X_1$–$P2X_7$) encoded by distinct genes (Surprenant et al., 1995; Khakh, 2001; North, 2002). These subunits can be assembled in various combinations to form homomeric or heteromeric receptors. Functional P2X receptors are most probably composed of three subunits (Nicke et al., 1998; Barrera et al., 2005; North and Verkhratsky, 2006). Immunoreactivity for $P2X_1$ receptors was detected in cerebellar astrocytes (Loesch and Burnstock, 1998), $P2X_2$ receptors were similarly detected in glial cells in the spinal cord (Kanjhan et al., 1999) and in pituicytes (Loesch et al., 1999), whereas immunoreactivity to $P2X_4$ receptors was found in astrocytes in the brainstem (Ashour and Deuchars, 2004). Astroglial

Received Dec. 9, 2007; revised April 8, 2008; accepted April 9, 2008.

This work was supported by The Wellcome Trust, the National Institutes of Health, the Alzheimer Research Trust (United Kingdom), the Deutsche Forschungsgemeinschaft (Center for Molecular Physiology of the Brain, Grant SPP 1172), and the Max Planck Society.

Correspondence should be addressed to Prof. Alexei Verkhratsky, Faculty of Life Sciences, The University of Manchester, 1.124 Stopford Building, Oxford Road, Manchester M13 9PT, UK. E-mail: alex.verkhratsky@manchester.ac.uk.

DOI:10.1523/JNEUROSCI.1149-08.2008

 0270-6474/08/285473-08$15.00/0

cells from nucleus accumbens possessed mRNA for $P2X_1$–$P2X_7$, whereas immunohistochemistry revealed the expression of only $P2X_2$, $P2X_3$, and $P2X_4$ subunits (Franke et al., 2001). Functional activity of P2X receptors was hitherto detected only in cultured astrocytes through identification of $^{45}Ca^{2+}$ entry (Neary et al., 1988) or ATP-induced membrane currents (Walz et al., 1994). In the present study, we performed a detailed investigation of the biophysical and pharmacological properties of ATP-induced membrane currents in astrocytes acutely isolated from cortical slices of transgenic mice with enhanced green fluorescent protein (EGFP)-expressing astroglial cells.

Materials and Methods

Acute isolation of astrocytes. Experiments were performed on transgenic mice expressing EGFP under the control of the human glial fibrillary acidic protein (GFAP) promoter [line TgN(GFAP-EGFP)GFEC-FKi]. This line has been generated similarly to the line [now designated TgN(GFAP-EGFP)GFEA-FKi] described for the first time by Nolte et al. (2001) and further studied (Matthias et al., 2003; Grass et al., 2004; Hirrlinger et al., 2004; Lalo et al., 2006).

Mice (10–22 d) were anesthetized by halothane and then decapitated, in accordance with United Kingdom legislation. Slices were prepared using the technique described previously (Lalo et al., 2006). Brains were rapidly dissected and placed in physiological saline containing the following (in mM): 135 NaCl, 3 KCl, 1 $MgCl_2$, 2.4 $CaCl_2$, 26 $NaHCO_3$, 1 NaH_2PO_4, and 15 glucose, pH 7.4 (when gassed with 95% O_2/5%CO_2). Brain slices (300 μm thick) were cut at 4°C and kept at room temperature for 1–2 h before the cell isolation.

Astrocytes were acutely isolated using the modified "vibrating ball" technique (Vorobjev, 1991) (see also Pankratov et al., 2002; Lalo et al., 2006). The glass ball (200 μm diameter) was moved slowly some 10–50 μm above the slice surface, while vibrating at 100 Hz (lateral displacements, 20–30 μm). The composition of external solution for isolated cell experiments was included the following (in mM): 135 NaCl, 2.7 KCl, 2.5 $CaCl_2$, 1 $MgCl_2$, 10 HEPES, 1 NaH_2PO_4, and 15 glucose, pH adjusted with NaOH to 7.3.

Identification of astrocytes. Astrocytes were identified by EGFP fluorescence. For this purpose, cells were illuminated at 490 nm and observed at 510 ± 10 nm. All cells identified visually demonstrated an electrophysiological signature characteristic of astrocytes. A series of depolarizing and hyperpolarizing voltage steps from a holding potential of −80 mV evoked passive currents, with nearly linear current–voltage (*I–V*) relationship as described by Lalo et al. (2006).

Electrophysiological recordings. Whole-cell voltage-clamp recordings from isolated astrocytes were made with patch pipettes (3.5–4 MΩ) filled with intracellular solution (in mM: 110 KCl, 10 NaCl, 10 HEPES, 5 MgATP, and 0.2 EGTA, pH 7.35). The membrane potential was clamped at −80 mV unless stated otherwise. Currents were monitored using an EPC-9 patch-clamp amplifier (HEKA) filtered at 3 kHz and stored on the disk for off-line analysis. Liquid junction potentials were measured with the EPC-9 patch-clamp amplifier and PULSE software (HEKA); all voltages reported were corrected accordingly. Recordings commenced 10 min after whole-cell access was gained, to ensure equilibration between the pipette solution and the cytosol. Series resistances were 4–12 MΩ, and input resistances were 50–100 MΩ; both varied by <20% in the cells accepted for analysis. A modified "square-pulse" concentration jump method (Lalo et al., 2001; Pankratov et al., 2003) was used for rapid (exchange time of ~5 ms) applications of solutions containing various agents to single cells. Antagonists and modulators of purinoreceptors [pyridoxal-phosphate-6-azophenyl-2′,4′-disulfonate (PPADS), ivermectin, and trinitrophenyl (TNP)-ATP] were preapplied for 2 min before application of agonists. Experiments were controlled by PULSE software (HEKA), and data were analyzed by self-designed software installed on a Windows NT workstation (Microsoft).

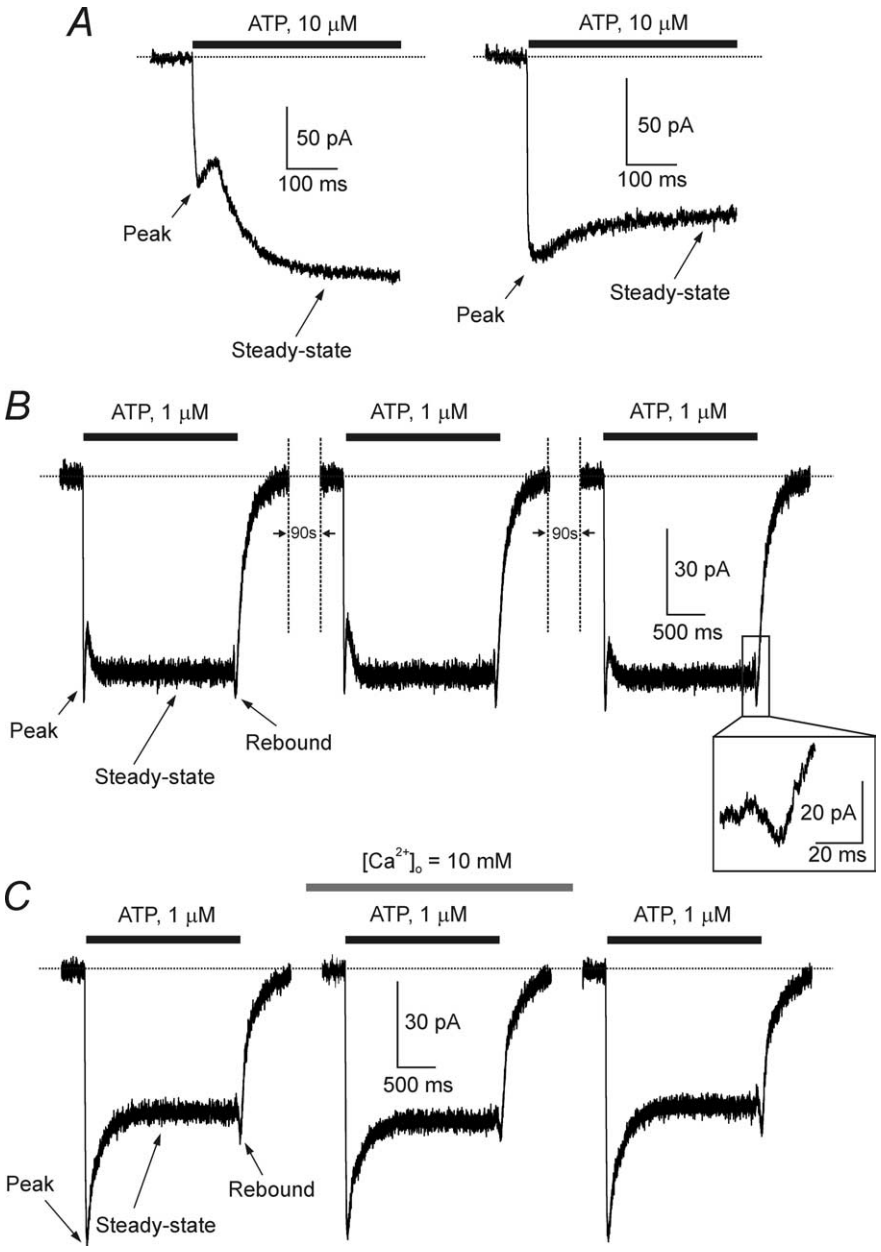

Figure 1. Kinetics and concentration dependences of ATP-induced currents in cortical astrocytes. ***A***, Examples of two types of ATP-induced currents, recorded from acutely isolated astrocytes. The left shows a type 1 response, observed in the majority of cells, and the right shows a type 2 response expressed in approximately one-third of all cells tested. ***B***, ATP currents evoked by repetitive applications of the agonist show no apparent desensitization. Current traces have a complex kinetics; the peak of the response, the steady-state component, and the rebound inward current recorded during ATP washout are indicated on the graph. ***C***, Increase in the extracellular Ca^{2+} concentration from 2.5 to 10 mM does not affect the ATP-induced currents. All recordings were made at a holding potential of −80 mV.

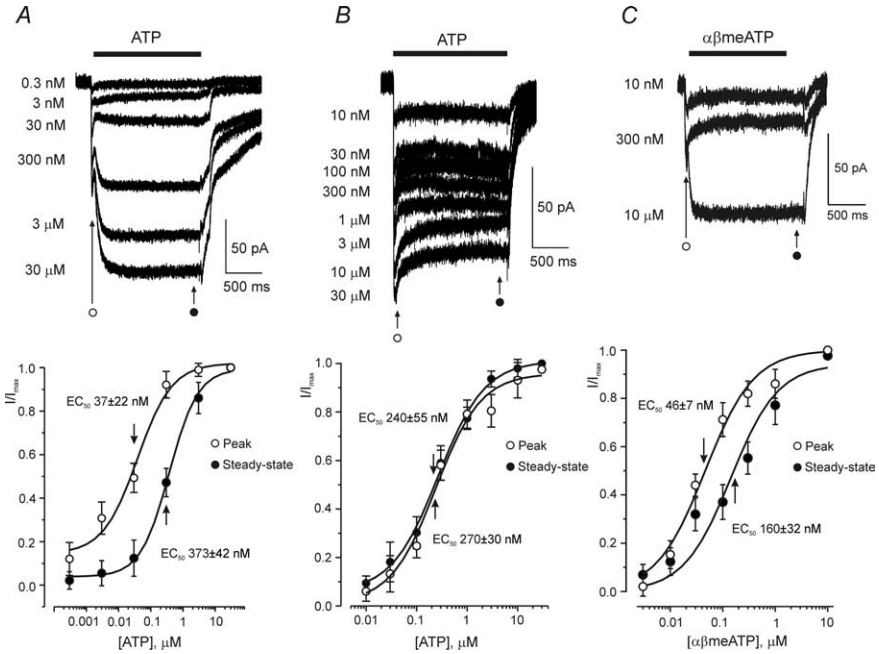

Figure 2. Concentration dependence of ATP-induced currents in cortical astrocytes. ***A***, Concentration dependence of peak and steady-state components of the type 1 ATP-induced response. Membrane currents recorded from a single cell in response to different ATP concentrations are shown on the top. The bottom shows the concentration–response curves constructed from nine similar experiments; current amplitudes were measured at the initial peak and at the end of the current, as indicated on the graph. ***B***, Concentration dependence of the type 2 ATP-induced response. The family of membrane currents evoked by various ATP concentrations is shown on the top. The concentration–response curves constructed for the peak and steady-state of the ATP-induced currents (as indicated on the graph) recorded from eight cells are represented in the bottom. ***C***, Membrane currents recorded from single astrocyte in response to different concentrations of $\alpha\beta$meATP are represented on the top; bottom shows the concentration–response curves for peak and steady-state currents; data were pooled from six experiments. All recordings were made at a holding potential of −80 mV.

Ex vivo *fluorescence-activated cell sorting of glial cell populations.* To isolate pure samples of astroglial cell populations, brains from transgenic GFAP–EGFP mice were isolated at postnatal day 6 (P6). Vibratome sections of cortices prepared from dissected brains were subjected to papain digestion according to the protocols of the manufacturer (Worthington). After 30 min incubation at 37°C in a humidified chamber, tissue samples were thoroughly homogenized with glass-polished Pasteur pipettes to yield homogenous solutions. Remaining tissue debris of larger size was collected by gravity, and the supernatant single-cell suspension was stained at 37°C for 30 min with the nuclear dyes propidium iodide (PI) and Hoechst 33342 to separate dead and alive cells (Invitrogen). Fluorescence-activated cell sorting (FACS) was performed using an FACS-Aria (Becton Dickinson) with gates set to obtain at least 10^5 PI-negative and Hoechst/GFP-positive cell bodies with a purity >99% as determined by subsequent microscopic control. Cells of interest were sorted directly into RLT RNA lysis buffer, and RNA preparation was performed with RNeasy Micro-Kits according to protocols given by the manufacturer (Qiagen). After elution of the total RNA with 100 μl of RNase-free water from the columns, the RNA was precipitated in the presence of pellet paint (EMD Chemicals) and resuspended in 5–10 μl of water. Aliquots were frozen at − 20°C and subsequently used for quantitative real-time (qRT)-PCR analysis.

qRT-PCR analysis. QRT-PCR was performed as described previously (Rossner et al., 2006). In brief, assays were performed using a 7500 Fast Sequence Detection System (Applied Biosystems) according to the 2-ΔΔCt method (Livak and Schmittgen, 2001). All ΔCt values were normalized to the expression of ATP5b (Andersen et al., 2004). Total RNA from isolated cells was reverse transcribed using Superscript III (Invitrogen). For qRT-PCR, the Power SYBR Green PCR Master Mix (Applied Biosystems) was used according to the instructions of the manufacturer. Intron-spanning primers close to the 3′ end of the transcripts were designed with the Universal Probe Library Assay Design Center (Roche Applied Science). The respective primer pairs were designed for mouse mRNAs (sequences are given in 5′–3′ direction; GenBank accession number in parentheses): $P2X_1$ (NM_008771.2), CCG AAG CCT TGC TGA GAA, GGT TTG CAG TGC CGT ACA T; $P2X_2$ (AY044240.2), ATG GGA TTC GAA TTG ACG TT, GAT GGT GGG AAT GAG ACT GAA; $P2X_3$ (ENSMUST00000028465.6), GGT GGC TGC CTT CAC TTC, TCA GCC CCT TTG AGG AAA; $P2X_4$ (AJ251459.1), CCA ACA CTT CTC AGC TTG GAT, TGG TCA TGA TGA AGA GGG AGT; $P2X_5$ (AF333331.1), CAC AGT CAT CAA CAT TGG TTC C, AGG TAG ATA AGT ACC AGG TCA CAG AAG; $P2X_6$ (NM_011028.1), TGT CCC CAG TAC TCC TTC CA, CAC CAG TGA TTG GCT GTC C; $P2X_7$ (AJ009823.1), GGG GGT TTA CCC CTA CTG TAA, GCT CGT CGA CAA AGG ACA C; ATP5B (NM_016774.2), GGC ACA ATG CAG GAA AGG, TCA GCA GGC ACA TAG ATA GCC; CALB1 (NM_009788.2), AAG GCT TTT GAG TTA TAT GAT CAG G, TTC TTC TCA CAC AGA TCT TTC AGC; ENO2 (NM_013509.2), TGG AGT TTG GGG AGT GCT GGA TG, AGG GCT GGG GAG AGG GTT AGA GG; GFAP (3) (NM_031166.1), TCA AGA GGA ACA TCG TGG TAA AGA, TGC TCC TGC TTC GAG TCC TT; ITGAM (Mac-1) (ENSMUST00000064821.3), TCC TGT TTA ATG ACT CTG CGT TT, GGC TCC ACT TTG GTC TCT GT.

Drugs. Unless specifically indicated all salts, chemicals, and reagents were from Sigma.

Results

ATP-induced currents

Recordings from visually identified, fluorescent astrocytes were made within 30–40 min after isolation. All the cells had current–voltage relationships close to linear (for general electrophysiology of acutely isolated cortical astrocytes, see Lalo et al., 2006). Application of ATP (1–10 μM) to the astrocytes voltage clamped at −80 mV evoked an inward current in 75 of 81 cells tested. ATP-induced currents showed complex time course with initial rapid and steady-state phases. The overall current kinetics fell into two classes among different cells. In 49 of 75 cells, the ATP-induced currents were clearly biphasic with an initial phase, which peaked rapidly and then showed some decay that was interrupted by a slower delayed phase (Fig. 1*A*,*B*). The rapid phase peaked in 22 ± 9 ms, after which it began to decay; the slower phase reached a maximal value 184 ± 45 ms after the beginning of the ATP application and displayed no obvious inactivation during 2 s of agonist application. In the second group of cells (26 of 75) (Fig. 1*A*,*C*) ATP evoked a smoother response with rapid peak (time to peak, 19 ± 7 ms) and slowly decaying plateau phase (decay time constant, 239 ± 47 ms). We classified these two classes of currents as "type 1" and "type 2" responses. The tail current for all types of currents induced by moderate ATP concentrations (1–3 μM), which was monitored immediately after rapid washout of the drug, also had a complex kinetic with transient inward ("rebound") component (Fig. 1). ATP-induced currents showed no desensitization in response to sequential applications of agonist with an inter-application interval of 90–150 s ($n = 7$) (Fig. 1*B*). Furthermore, ATP-induced currents were not affected by increasing the extracellular Ca^{2+} concentration from

usual 2.5 to 10 mM ($n = 4$) (Fig. 1*C*). We used application interval of 150 s as a standard in all additional experiments.

ATP-induced currents were concentration dependent. In the cells having type 1 responses, the two phases of the current had a different sensitivity to ATP (Fig. 2*A*). The rapid phase was activated at lower concentrations (EC_{50} of 37 ± 22 nM; $n = 9$). The EC_{50} for the slow component was ~10 times higher (373 ± 42 nM; $n = 9$). The Hill slopes were 0.88 ± 0.08 and 0.97 ± 0.05 ($n = 9$) for fast and slow component, respectively. In cells with type 2 response, the dose–response curves constructed for the peak current value and for the current value at the end of ATP application were similar, with EC_{50} values of 240 ± 55 and 270 ± 30 nM, respectively ($n = 8$) (Fig. 2*B*); the Hill slopes were 0.97 ± 0.06 and 0.99 ± 0.07 ($n = 8$). Application of a P2X receptors agonist, $\alpha\beta$methylene ATP ($\alpha\beta$meATP) (Gever et al., 2006), triggered a type 1 response in 15 cells tested (Fig. 2*C*) and a type 2 response in five cells tested. The rapid component of the type 1 response was activated with an EC_{50} of 46 ± 7 nM, whereas the slow component with an EC_{50} of 160 ± 32 nM ($n = 6$).

The *I–V* relationships for the ATP-induced currents were constructed from families of currents recorded at different holding potentials in response to the application of fixed concentrations of ATP (3 and 10 μM). The *I–V* curves were linear for all types of the responses and had a reversal potential (Fig. 3) of 4.4 ± 1.6 mV ($n = 10$).

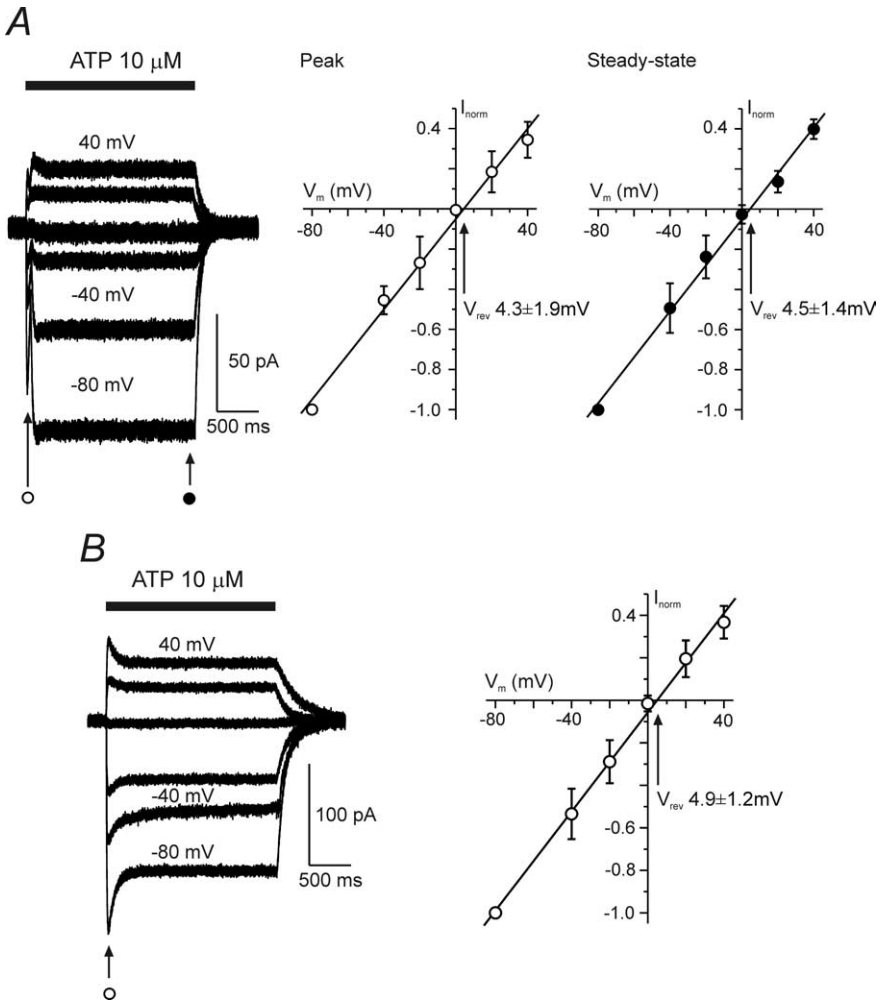

Figure 3. Voltage dependence of the ATP-induced currents. ***A*** and ***B*** show the voltage dependence of the type 1 (***A***) and type 2 (***B***) ATP-induced currents. The left panels demonstrate families of ion currents evoked by ATP at holding potentials varying between −80 and 40 mV. Current–voltage plots for ATP-induced currents are shown on the right (***A***, $n = 6$; ***B***, $n = 7$). The amplitudes of currents were normalized to the value measured at −80 mV.

The biphasic kinetics of the ATP-induced current recorded from some astrocytes somewhat resembled currents generated during the dilation of certain types of P2X receptors in the presence of agonist (Khakh et al., 1999b; Virginio et al., 1999). This dilation of the channel pore rapidly increases the permeability of the P2X receptor for larger cations, which may underlie the generation of the delayed current component. To address this possibility, we substituted the extracellular cations with *N*-methyl-D-glucamine (NMDG) and then applied ATP. In its initial state, P2X receptor is not permeable to NMDG, and removal of small cations should eliminate ionic current through P2X receptors completely. During pore dilation, the permeability to NMDG would gradually build up, resulting in the slow-developing inward current. Under these conditions, however, ATP failed to produce an inward current ($n = 12$; data not shown), which argues against the appearance of the channel pore dilation.

The ATP-induced currents were completely inhibited by the P2X receptor antagonist PPADS (Gever et al., 2006); however, the sensitivity of the current components was different. In cells with a type 1 response, PPADS blocked the rapid current with an IC_{50} of 0.7 ± 0.5 μM, whereas the slow component was suppressed with an IC_{50} of 8.6 ± 0.9 μM ($n = 9$) (Fig. 4*A*). In cells with type 2 responses, the ATP-induced currents were blocked by PPADS, with an IC_{50} of 0.5 ± 0.3 μM for the peak component and 4.7 ± 0.5 μM for the steady-state component ($n = 7$) (Fig. 4*B*). It should be noted that different sensitivity of peak and steady-state components to PPADS may be explained by potentiation of plateau current by low concentrations of PPADS, similar to the effect observed by Haines et al. (1999).

Furthermore, the ATP-induced currents were blocked by TNP-ATP, the specific antagonist of $P2X_{1/5}$ heteromeric receptors (Haines et al., 1999; Surprenant et al., 2000). The inhibition of ATP (1 μM) induced currents was concentration dependent (Fig. 5); 1 μM TNP-ATP present in the extracellular solution produced ~90% inhibition. TNP-ATP blocked both type 1 ($n = 6$) and type 2 ($n = 3$) responses with equal potency.

In contrast, the selective positive modulator of $P2X_4$ receptors, ivermectin (Khakh et al., 1999a; Priel and Silberberg, 2004; Lalo et al., 2007) at 1–10 μM, had no effect on ATP-induced currents in acutely isolated astrocytes (Fig. 6). In all 14 cells tested, ivermectin failed to modulate the current responses evoked by application of ATP; this was the case for both types of ATP responses, the type 1 ($n = 8$) and type 2 ($n = 6$).

Identification of P2X receptor transcripts in FACS-sorted astrocytes by quantitative real-time PCR

To quantify the expression of P2X receptors and to determine the identity of P2X receptor subunits, qRT-PCR was performed on

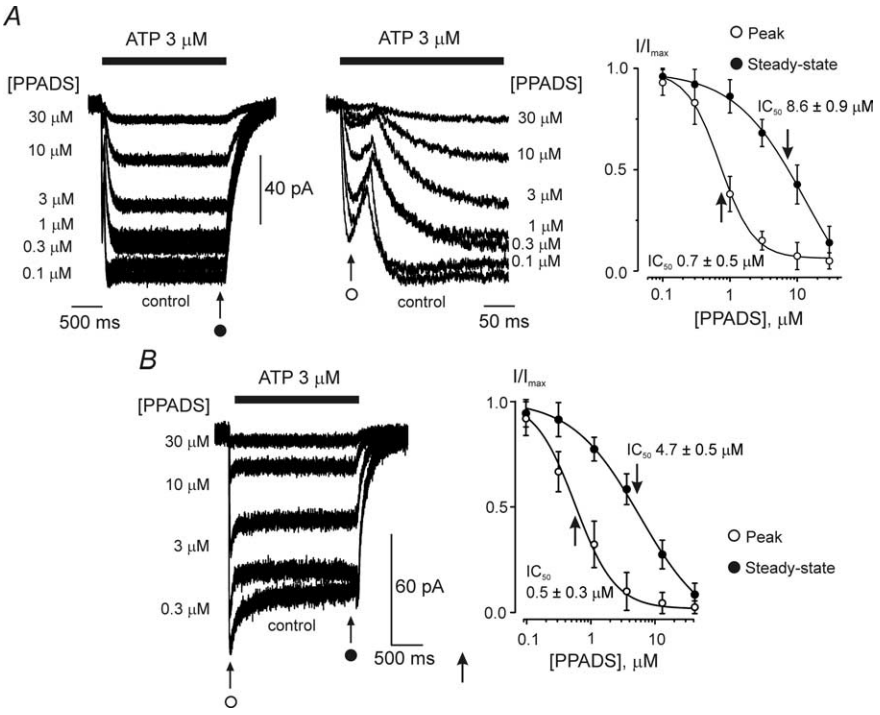

Figure 4. Inhibition of ATP-induced currents by PPADS. ***A***, PPADS sensitivity of type 1 ATP-induced responses. The left panel demonstrates the family of currents triggered by 3 μM ATP in control conditions and in the presence of various concentrations of PPADS, as indicated. Membrane currents are shown at two different timescales. The right panel shows the concentration dependence of the block for nine cells; the peak component of the response is considerably more sensitive to PPADS. ***B***, PPADS sensitivity of type 2 ATP-induced responses. Currents recorded at various concentrations of PPADS are shown on the left, and the concentration dependence of inhibition for peak and steady-state components constructed for seven individual experiments is presented on the right. Similarly to currents shown in ***A***, the peak component of the response was more sensitive to PPADS. Application of PPADS started 2 min before application of ATP. All recordings were made at a holding potential of −80 mV.

purified astrocytes. Cells were FACS sorted from the cortex of postnatal TgN(GFAP–EGFP) mice, and the results were compared with the total cortex of wild-type mice (Fig. 7). The mRNA expression levels of P2X receptor subunits of astrocytes and of total cortex tissue were normalized (set to unity) to the expression level of the β subunit of the ATP synthase (ATP5B, a part of the mitochondrial F1 complex). This gene has been shown to be homogenously distributed in 12 different human tissues, including brain (Andersen et al., 2004). The qRT-PCR analysis shows that mRNAs for $P2X_1$ and $P2X_5$ are expressed at very high levels in astrocytes. Small amounts of $P2X_2$ message can also be detected. The expression levels of the other P2X receptor subunits were negligible. Control experiments performed on FACS-purified microglial cells of TgH(CX3CR1–EGFP) mice (Jung et al., 2000) revealed that the astroglial cDNA was very pure, with only minor contaminations (supplemental Fig. 1, available at www.jneurosci.org as supplemental material), further strengthening the validity of the qRT-PCR analysis.

Discussion

ATP plays an important role in signal transfer between neuronal and glial circuits and within glial networks (Verkhratsky and Steinhauser, 2000; Fields and Burnstock, 2006; North and Verkhratsky, 2006). ATP acts as a widespread gliotransmitter; when released from glia, ATP triggers and maintains glial calcium signals and calcium waves (Cotrina et al., 2000; Volterra and Meldolesi, 2005) as well as signals to the neurons (Zhang et al., 2003; Pascual et al., 2005). Glial cells express a variety of P2 receptors, which are activated by ATP released from either neighboring glia or neuronal terminals during synaptic transmission. Although properties of ionotropic P2X ion currents are well characterized in microglia (Farber and Kettenmann, 2006), their detailed characterization in astrocytes and oligodendrocytes is yet to be established. ATP-mediated ion currents were detected in cultured astroglia (Walz et al., 1994); it has to be noted, however, that expression of receptors in cultured astrocytes may not necessarily reflect the situation *in situ*; this is because of plasticity of astroglial cells, which may considerably affect receptors expression in the *in vitro* systems (Verkhratsky et al., 1998; Verkhratsky and Steinhauser, 2000).

The main problem in characterization of astroglial P2X receptors and P2X-mediated ion currents *in situ* is associated with the slice preparation per se. Our own preliminary experiments, as well as experience of other groups, indicated that application of exogenous ATP to astrocytes in slices elicited rather unpredictable and often nonreproducible current responses. Recording of ATP-induced currents required application of very high (~1 mM) concentrations of the agonist, and, in most cases, only the first application evoked a response; subsequent stimulation of astrocytes with ATP did not produce currents even after long (up to 20 min) periods of washout with control solution. This may result from diffusion barriers, rapid desensitization of the receptors, ATP breakdown by nucleotidases, or a combination of the above. Furthermore, expression of P2X receptors can vary substantially between brain regions, and indeed Jabs et al. (2007) were not able to identify any P2X-mediated currents in hippocampal astrocytes.

The use of astrocytes acutely isolated from cortical slices has now allowed reliable recording of ATP-induced currents. For cell isolation, we used a mechanical dissociation technique, which eliminated any possible effects of enzymes on membrane receptors. Furthermore, the single-cell preparation allowed us to use an extracellular concentration clamp, which offers a precise control over concentration of the ligand and duration of its application. The use of transgenic mice, in which the fluorescent indicator EGFP was confined to astrocytes, facilitated the identification of astrocytes. In addition, electrophysiological analysis revealed whole-cell membrane currents characteristic of astrocytes.

We found that almost all astrocytes acutely isolated from cortex are responsive to application of ATP in nanomolar to micromolar concentrations. The currents generated by ATP in astroglial cells displayed several unique properties. First, they show an exceptional sensitivity to the agonist, being fully activated by low micromolar ATP concentrations. Second, the ATP-induced currents have complex kinetics with clearly identified rapid and sustained components. In the majority of cells, ATP evoked a biphasic response, comprising a rapid initial and a delayed steady-state component; these components were differentially sensitive to the agonist, the rapid one being fully activated at ~1 μM ATP, whereas the delayed component was ~10 times less sensitive. The second type of the ATP-induced response, detected in approxi-

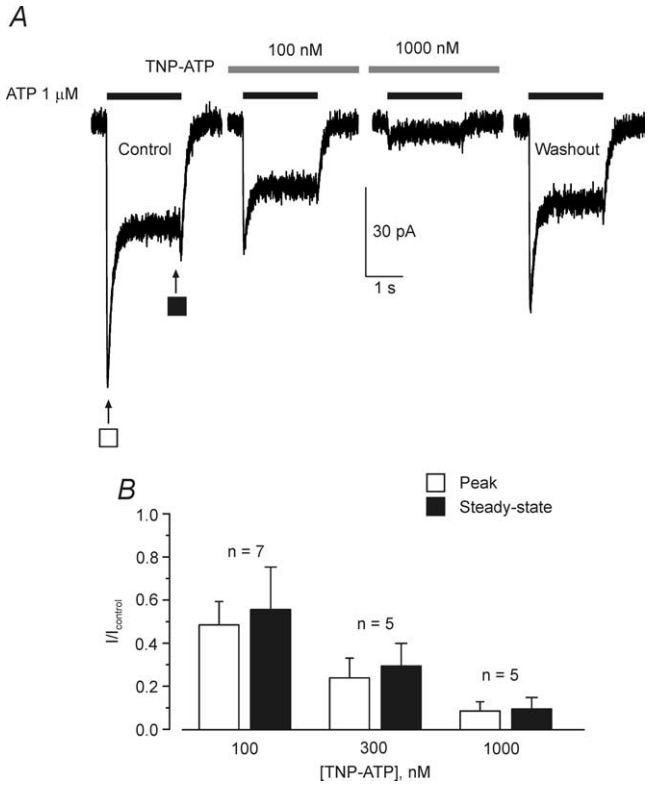

Figure 5. Inhibition of ATP-induced currents by TNP-ATP. ***A***, ATP-induced current measured for the cortical astrocytes in control conditions, in the presence of TNP-ATP, and after the washout. ***B***, Mean data showing the percentage of ATP-induced current inhibition at three different concentrations of TNP-ATP; the number of experiments is shown on the graph. Application of TNP-ATP started 2 min before application of ATP. All recordings were made at a holding potential of −80 mV.

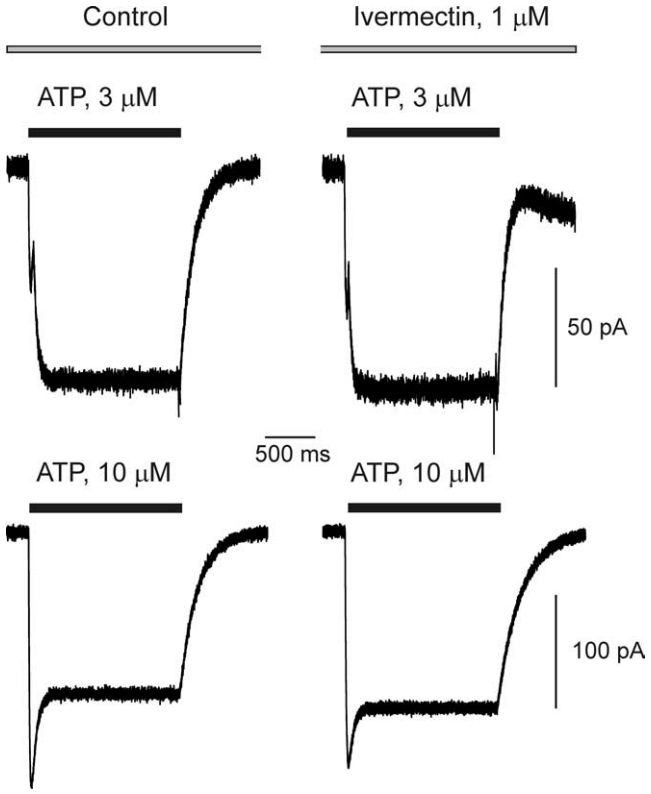

Figure 6. Ivermectin does not affect ATP-induced currents. Type 1 (top) and type 2 ATP-induced responses recorded in control conditions and in the presence of the positive modulator of P2X$_4$ receptor ivermectin. The holding potential was −80 mV.

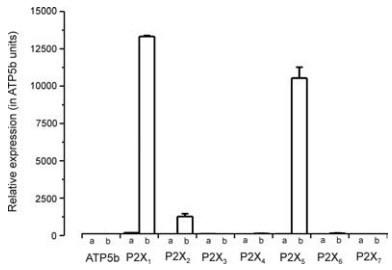

Figure 7. Quantitative real-time PCR analysis to identify mRNAs for P2X receptor subunits and their relative expression levels. Samples of mRNA were prepared from total mouse cortex (a) or from FACS-sorted cortical astrocytes (b) of postnatal mice (P6) and were subjected to qRT-PCR. Data represent mRNA levels relative to ATP5B and are given in means ± SEM.

mately one-third of the cells, also had a clearly defined initial peak and steady-state components. This current was fully activated at ATP concentrations >10 μM. Both types of ATP responses were associated with an opening of distinct ATP-gated channels and not with any "dilation" of the P2X receptors. The current–voltage relationships for both types of ATP-induced currents were linear, with a reversal potential ~5 mV; this is characteristic for P2X cationic channels. Third, the kinetics of the ATP responses was peculiar because in many cases the decay of the current after agonist washout was interrupted by a transient rebound inward current. Fourth, the ATP currents were resistant to the desensitization in response to sequential applications of the agonist with short intervals. Fifth, similar responses, demonstrating the rebound tail currents and no desensitization were evoked by αβmeATP. Sixth, the ATP-induced ion currents were effectively blocked by PPADS and TNP-ATP.

All these properties are characteristic for only one class of P2X receptors, the P2X$_{1/5}$ heteromeric receptors. Functional heteromeric P2X$_{1/5}$ currents were hitherto investigated only in artificial expression systems [oocytes, HEK, COS-7, and CHO cells (Torres et al., 1998; Haines et al., 1999; Le et al., 1999; Surprenant et al., 2000)], with no evidence for P2X$_{1/5}$ receptors operative in native cells. Responses mediated by heteromeric P2X$_{1/5}$ receptors show several unique features: (1) a very high sensitivity to ATP (3–10 nM ATP already evoked measurable currents); (2) biphasic kinetics with distinct peak and steady-state components; (3) rebound currents monitored after washout of the agonist; (4) no desensitization in response to the repetitive agonist applications; (5) sensitivity to αβmeATP; and (6) effective inhibition by PPADS and TNP-ATP. All these features therefore are strikingly similar to the properties of ATP-mediated currents in cortical astrocytes.

The idea of the functional expression of P2X$_{1/5}$ receptors in astroglial cells was further corroborated by our qRT-PCR experiments, which demonstrated high expression of mRNA for P2X$_1$ and P2X$_5$, with only marginal expression of P2X$_2$ subunit mRNAs in cortical astrocytes. Based on the data discussed above, we may therefore suggest that cortical astrocytes are endowed with functional heteromeric P2X$_{1/5}$ receptors, a combination that has not previously been discovered in native cells. Two distinct types of kinetics of ATP-evoked currents are probably associated with variability in heteromeric assembly of P2X$_{1/5}$ subunits. We could not detect expression of P2X$_4$ subunits mRNAs, which correlated with observed insensitivity of the ATP-mediated currents to the

positive modulator of $P2X_4$, ivermectin. Furthermore, brain astrocytes do not show expression of $P2X_7$ receptors. Additional experiments, in particular, those taking advantage of mouse transgenic models with selective modulation of astroglial P2X expression, will be necessary to evaluate the impact of glial P2X-mediated signaling.

The P2X receptors residing in astroglial membrane might be activated by ATP from two distinct sources. ATP can be released from either presynaptic terminals or astrocytes themselves. Synaptic release of ATP in cortex occurs by a vesicular pathway (Pankratov et al., 2006, 2007); similarly, ATP can be released with other gliotransmitters from astrocytes (Volterra and Meldolesi, 2005). The synaptic release of ATP in the cortex occurs from glutamatergic terminals (Pankratov et al., 2007), so perisynaptic astrocytes could perceive both neurotransmitters (ATP and glutamate) simultaneously (Verkhratsky and Kirchhoff, 2007a,b). Activation of respective glial receptors can be functionally relevant for the plastic potential of neuronal–glial communication at the level of cortical synapse.

References

Andersen CL, Jensen JL, Orntoft TF (2004) Normalization of real-time quantitative reverse transcription-PCR data: a model-based variance estimation approach to identify genes suited for normalization, applied to bladder and colon cancer data sets. Cancer Res 64:5245–5250.

Ashour F, Deuchars J (2004) Electron microscopic localisation of $P2X_4$ receptor subunit immunoreactivity to pre- and post-synaptic neuronal elements and glial processes in the dorsal vagal complex of the rat. Brain Res 1026:44–55.

Barrera NP, Ormond SJ, Henderson RM, Murrell-Lagnado RD, Edwardson JM (2005) Atomic force microscopy imaging demonstrates that $P2X_2$ receptors are trimers but that $P2X_6$ receptor subunits do not oligomerize. J Biol Chem 280:10759–10765.

Bowser DN, Khakh BS (2004) ATP excites interneurons and astrocytes to increase synaptic inhibition in neuronal networks. J Neurosci 24:8606–8620.

Burnstock G (1972) Purinergic nerves. Pharmacol Rev 24:509–581.

Burnstock G (1977) The purinergic nerve hypothesis. Ciba Found Symp 48:295–314.

Burnstock G (2004) 50 years of passionate commitment. Cell Mol Life Sci 61:1693–1696.

Cotrina ML, Lin JH, Nedergaard M (1998) Cytoskeletal assembly and ATP release regulate astrocytic calcium signaling. J Neurosci 18:8794–8804.

Cotrina ML, Lin JH, Lopez-Garcia JC, Naus CC, Nedergaard M (2000) ATP-mediated glia signaling. J Neurosci 20:2835–2844.

Edwards FA, Gibb AJ, Colquhoun D (1992) ATP receptor-mediated synaptic currents in the central nervous system. Nature 359:144–147.

Edwards FA, Robertson SJ, Gibb AJ (1997) Properties of ATP receptor-mediated synaptic transmission in the rat medial habenula. Neuropharmacology 36:1253–1268.

Egan TM, Samways DS, Li Z (2006) Biophysics of P2X receptors. Pflügers Arch 452:501–512.

Erb L, Liao Z, Seye CI, Weisman GA (2006) P2 receptors: intracellular signaling. Pflügers Arch 452:552–562.

Farber K, Kettenmann H (2006) Purinergic signaling and microglia. Pflügers Arch 452:615–621.

Fellin T, Pozzan T, Carmignoto G (2006) Purinergic receptors mediate two distinct glutamate release pathways in hippocampal astrocytes. J Biol Chem 281:4274–4284.

Fields RD, Burnstock G (2006) Purinergic signalling in neuron-glia interactions. Nat Rev Neurosci 7:423–436.

Franke H, Grosche J, Schadlich H, Krugel U, Allgaier C, Illes P (2001) P2X receptor expression on astrocytes in the nucleus accumbens of rats. Neuroscience 108:421–429.

Gever JR, Cockayne DA, Dillon MP, Burnstock G, Ford AP (2006) Pharmacology of P2X channels. Pflügers Arch 452:513–537.

Grass D, Pawlowski PG, Hirrlinger J, Papadopoulos N, Richter DW, Kirchhoff F, Hulsmann S (2004) Diversity of functional astroglial properties in the respiratory network. J Neurosci 24:1358–1365.

Haas S, Brockhaus J, Verkhratsky A, Kettenmann H (1996) ATP-induced membrane currents in ameboid microglia acutely isolated from mouse brain slices. Neuroscience 75:257–261.

Haines WR, Torres GE, Voigt MM, Egan TM (1999) Properties of the novel ATP-gated ionotropic receptor composed of the $P2X_1$ and $P2X_5$ isoforms. Mol Pharmacol 56:720–727.

Hirrlinger J, Hulsmann S, Kirchhoff F (2004) Astroglial processes show spontaneous motility at active synaptic terminals in situ. Eur J Neurosci 20:2235–2239.

Hussl S, Boehm S (2006) Functions of neuronal P2Y receptors. Pflügers Arch 452:538–551.

Jabs R, Matthias K, Grote A, Grauer M, Seifert G, Steinhauser C (2007) Lack of P2X receptor mediated currents in astrocytes and GluR type glial cells of the hippocampal CA1 region. Glia 55:1648–1655.

James G, Butt AM (2001) P2X and P2Y purinoreceptors mediate ATP-evoked calcium signalling in optic nerve glia in situ. Cell Calcium 30:251–259.

Jung S, Aliberti J, Graemmel P, Sunshine MJ, Kreutzberg GW, Sher A, Littman DR (2000) Analysis of fractalkine receptor CX_3CR1 function by targeted deletion and green fluorescent protein reporter gene insertion. Mol Cell Biol 20:4106–4114.

Kanjhan R, Housley GD, Burton LD, Christie DL, Kippenberger A, Thorne PR, Luo L, Ryan AF (1999) Distribution of the $P2X_2$ receptor subunit of the ATP-gated ion channels in the rat central nervous system. J Comp Neurol 407:11–32.

Khakh BS (2001) Molecular physiology of P2X receptors and ATP signalling at synapses. Nat Rev Neurosci 2:165–174.

Khakh BS, Proctor WR, Dunwiddie TV, Labarca C, Lester HA (1999a) Allosteric control of gating and kinetics at $P2X_4$ receptor channels. J Neurosci 19:7289–7299.

Khakh BS, Bao XR, Labarca C, Lester HA (1999b) Neuronal P2X transmitter-gated cation channels change their ion selectivity in seconds. Nat Neurosci 2:322–330.

King BF, Neary JT, Zhu Q, Wang S, Norenberg MD, Burnstock G (1996) P2 purinoceptors in rat cortical astrocytes: expression, calcium-imaging and signalling studies. Neuroscience 74:1187–1196.

Kirischuk S, Scherer J, Kettenmann H, Verkhratsky A (1995a) Activation of P2-purinoreceptors triggered Ca^{2+} release from $InsP_3$-sensitive internal stores in mammalian oligodendrocytes. J Physiol (Lond) 483:41–57.

Kirischuk S, Moller T, Voitenko N, Kettenmann H, Verkhratsky A (1995b) ATP-induced cytoplasmic calcium mobilization in Bergmann glial cells. J Neurosci 15:7861–7871.

Koizumi S, Fujishita K, Tsuda M, Shigemoto-Mogami Y, Inoue K (2003) Dynamic inhibition of excitatory synaptic transmission by astrocyte-derived ATP in hippocampal cultures. Proc Natl Acad Sci USA 100:11023–11028.

Lalo U, Pankratov Y, Kirchhoff F, North RA, Verkhratsky A (2006) NMDA receptors mediate neuron-to-glia signaling in mouse cortical astrocytes. J Neurosci 26:2673–2683.

Lalo U, Verkhratsky A, Pankratov Y (2007) Ivermectin potentiates ATP-induced ion currents in cortical neurones: evidence for functional expression of $P2X_4$ receptors? Neurosci Lett 421:158–162.

Lalo UV, Pankratov YV, Arndts D, Krishtal OA (2001) Omega-conotoxin GVIA potently inhibits the currents mediated by P2X receptors in rat DRG neurons. Brain Res Bull 54:507–512.

Le KT, Boue-Grabot E, Archambault V, Seguela P (1999) Functional and biochemical evidence for heteromeric ATP-gated channels composed of $P2X_1$ and $P2X_5$ subunits. J Biol Chem 274:15415–15419.

Livak KJ, Schmittgen TD (2001) Analysis of relative gene expression data using real-time quantitative PCR and the 2(-Delta Delta C(T)) Method. Methods 25:402–408.

Loesch A, Burnstock G (1998) Electron-immunocytochemical localization of $P2X_1$ receptors in the rat cerebellum. Cell Tissue Res 294:253–260.

Loesch A, Miah S, Burnstock G (1999) Ultrastructural localisation of ATP-gated $P2X_2$ receptor immunoreactivity in the rat hypothalamo-neurohypophysial system. J Neurocytol 28:495–504.

Matthias K, Kirchhoff F, Seifert G, Huttmann K, Matyash M, Kettenmann H, Steinhauser C (2003) Segregated expression of AMPA-type glutamate receptors and glutamate transporters defines distinct astrocyte populations in the mouse hippocampus. J Neurosci 23:1750–1758.

Moller T, Kann O, Verkhratsky A, Kettenmann H (2000) Activation of mouse microglial cells affects P2 receptor signaling. Brain Res 853:49–59.

Mori M, Heuss C, Gahwiler BH, Gerber U (2001) Fast synaptic transmission mediated by P2X receptors in CA3 pyramidal cells of rat hippocampal slice cultures. J Physiol (Lond) 535:115–123.

Neary JT, van Breemen C, Forster E, Norenberg LO, Norenberg MD (1988) ATP stimulates calcium influx in primary astrocyte cultures. Biochem Biophys Res Commun 157:1410–1416.

Nicke A, Baumert HG, Rettinger J, Eichele A, Lambrecht G, Mutschler E, Schmalzing G (1998) $P2X_1$ and $P2X_3$ receptors form stable trimers: a novel structural motif of ligand-gated ion channels. EMBO J 17:3016–3028.

Nieber K, Poelchen W, Illes P (1997) Role of ATP in fast excitatory synaptic potentials in locus coeruleus neurones of the rat. Br J Pharmacol 122:423–430.

Nolte C, Matyash M, Pivneva T, Schipke CG, Ohlemeyer C, Hanisch UK, Kirchhoff F, Kettenmann H (2001) GFAP promoter-controlled EGFP-expressing transgenic mice: a tool to visualize astrocytes and astrogliosis in living brain tissue. Glia 33:72–86.

North RA (2002) Molecular physiology of P2X receptors. Physiol Rev 82:1013–1067.

North RA, Verkhratsky A (2006) Purinergic transmission in the central nervous system. Pflügers Arch 452:479–485.

Pankratov Y, Castro E, Miras-Portugal MT, Krishtal O (1998) A purinergic component of the excitatory postsynaptic current mediated by P2X receptors in the CA1 neurons of the rat hippocampus. Eur J Neurosci 10:3898–3902.

Pankratov Y, Lalo U, Krishtal O, Verkhratsky A (2002) Ionotropic P2X purinoreceptors mediate synaptic transmission in rat pyramidal neurones of layer II/III of somato-sensory cortex. J Physiol (Lond) 542:529–536.

Pankratov Y, Lalo U, Krishtal O, Verkhratsky A (2003) P2X receptor-mediated excitatory synaptic currents in somatosensory cortex. Mol Cell Neurosci 24:842–849.

Pankratov Y, Lalo U, Verkhratsky A, North RA (2006) Vesicular release of ATP at central synapses. Pflügers Arch 452:589–597.

Pankratov Y, Lalo U, Verkhratsky A, North RA (2007) Quantal release of ATP in mouse cortex. J Gen Physiol 129:257–265.

Pascual O, Casper KB, Kubera C, Zhang J, Revilla-Sanchez R, Sul JY, Takano H, Moss SJ, McCarthy K, Haydon PG (2005) Astrocytic purinergic signaling coordinates synaptic networks. Science 310:113–116.

Priel A, Silberberg SD (2004) Mechanism of ivermectin facilitation of human $P2X_4$ receptor channels. J Gen Physiol 123:281–293.

Roberts JA, Vial C, Digby HR, Agboh KC, Wen H, Atterbury-Thomas A, Evans RJ (2006) Molecular properties of P2X receptors. Pflügers Arch 452:486–500.

Rossner MJ, Hirrlinger J, Wichert SP, Boehm C, Newrzella D, Hiemisch H, Eisenhardt G, Stuenkel C, von Ahsen O, Nave KA (2006) Global transcriptome analysis of genetically identified neurons in the adult cortex. J Neurosci 26:9956–9966.

Salter MW, Hicks JL (1994) ATP-evoked increases in intracellular calcium in neurons and glia from the dorsal spinal cord. J Neurosci 14:1563–1575.

Stout CE, Costantin JL, Naus CC, Charles AC (2002) Intercellular calcium signaling in astrocytes via ATP release through connexin hemichannels. J Biol Chem 277:10482–10488.

Surprenant A, Buell G, North RA (1995) P2X receptors bring new structure to ligand-gated ion channels. Trends Neurosci 18:224–229.

Surprenant A, Schneider DA, Wilson HL, Galligan JJ, North RA (2000) Functional properties of heteromeric $P2X_{1/5}$ receptors expressed in HEK cells and excitatory junction potentials in guinea-pig submucosal arterioles. J Auton Nerv Syst 81:249–263.

Torres GE, Haines WR, Egan TM, Voigt MM (1998) Co-expression of $P2X_1$ and $P2X_5$ receptor subunits reveals a novel ATP-gated ion channel. Mol Pharmacol 54:989–993.

Verderio C, Matteoli M (2001) ATP mediates calcium signaling between astrocytes and microglial cells: modulation by IFN-gamma. J Immunol 166:6383–6391.

Verkhratsky A, Kettenmann H (1996) Calcium signalling in glial cells. Trends Neurosci 19:346–352.

Verkhratsky A, Kirchhoff F (2007a) NMDA receptors in glia. Neuroscientist 13:28–37.

Verkhratsky A, Kirchhoff F (2007b) Glutamate-mediated neuronal-glial transmission. J Anat 210:651–660.

Verkhratsky A, Steinhauser C (2000) Ion channels in glial cells. Brain Res Brain Res Rev 32:380–412.

Verkhratsky A, Orkand RK, Kettenmann H (1998) Glial calcium: homeostasis and signaling function. Physiol Rev 78:99–141.

Virginio C, MacKenzie A, Rassendren FA, North RA, Surprenant A (1999) Pore dilation of neuronal P2X receptor channels. Nat Neurosci 2:315–321.

Volterra A, Meldolesi J (2005) Astrocytes, from brain glue to communication elements: the revolution continues. Nat Rev Neurosci 6:626–640.

Vorobjev VS (1991) Vibrodissociation of sliced mammalian nervous tissue. J Neurosci Methods 38:145–150.

Walz W, Gimpl G, Ohlemeyer C, Kettenmann H (1994) Extracellular ATP-induced currents in astrocytes: involvement of a cation channel. J Neurosci Res 38:12–18.

Zhang JM, Wang HK, Ye CQ, Ge W, Chen Y, Jiang ZL, Wu CP, Poo MM, Duan S (2003) ATP released by astrocytes mediates glutamatergic activity-dependent heterosynaptic suppression. Neuron 40:971–982.